Journal of Microscopy, Vol. 185, Pt 1, January 1997, pp. 67–75.
Received 1 November 1995; accepted 13 September 1996

A new method for the model-independent assessment of thickness in three-dimensional images

T. HILDEBRAND & P. RÜEGSEGGER
Institute for Biomedical Engineering, University of Zürich and Swiss Federal Institute of Technology (ETH), Moussonstrasse 18, CH-8044 Zürich, Switzerland

Key words. Distance transformation, mean thickness, micro-CT, stereology, structural parameters, thickness distribution, three-dimensional morphometry, trabecular bone structure.

Summary

Three-dimensional (3-D) structural parameters derived from lower-dimensional measurements using indirect morphometric methods may be strongly biased if the measured objects deviate from the assumed structure model. With the introduction of 3-D microscopic measuring techniques it is possible to obtain a complete depiction of complex spatial structures. As a consequence, new 3-D methods have recently been developed for the estimation of morphometric parameters such as volume, surface area and connectivity by direct processing of the 3-D images. Structure thickness is an important morphometric parameter which is usually defined for specific structure models only. In this paper we propose a general thickness definition for arbitrary structures allowing us to calculate the mean structure thickness and the thickness distribution of 3-D objects in a direct way and independently of an assumed structure model. Additionally, an efficient implementation for the practical usage of the method is described using distance transformation. The new method is applied to trabecular bone structures measured with a 3-D micro-computed tomography system.

1. Introduction

The problem addressed in this paper is the assessment of the mean structure thickness and thickness distribution in a direct and three-dimensional (3-D) way independently of the structure type.

Traditionally, stereological methods are used to derive 3-D morphometric parameters from 2-D measured sections of a sample. Stereology deals with the estimation of geometrical quantities of spatial objects from lower-dimensional probes and it has been thoroughly investigated and constantly refined since the introduction of the science in the 1960s (for a review of traditional stereological methods see Weibel, 1980; for recently developed methods see Gundersen *et al.*, 1988a,b; Cruz-Orive & Weibel, 1990).

To assess parameters like structure thickness and separation from measurements on 2-D sections special equations must be derived for different kinds of structure types. The mean structure thickness can be derived for example from perimeter and area assessments on a two-dimensionally measured section assuming a plate-like structure (Whitehouse, 1974). If the structure differs from the assumed type the calculated values will be biased to an unknown extent.

Several new measuring techniques make it possible to assess microstructures in a truly 3-D way nondestructively. Examples of such techniques are confocal fluorescence microscopy (Wijnaends van Resandt *et al.*, 1985; Wilson, 1990), micro-computed tomography (micro-CT) (Feldkamp *et al.*, 1989; Rüegsegger *et al.*, 1996) and micro-magnetic resonance imaging (Jara *et al.*, 1993).

Stereological equations can be 'extended' to three dimensions by going back to the original definitions. In the case of mean plate thickness, the 2-D measures perimeter and structure area can be exchanged with 3-D surface area and structure volume leading to a different but similar equation (Weibel, 1963). The necessary structure volume and surface area can be estimated directly from 3-D images using newly developed techniques (Guilak, 1994). Another stereological approach to calculate the mean structure thickness in both two and three dimensions is based on mean intercept length assessment (Weibel & Knight, 1964; Gundersen *et al.*, 1978; Cruz-Orive, 1979). The advantage with such 3-D techniques is that no assumptions regarding structure orientation are required because sample planes or test lines can always be chosen uniformly orientated in the 3-D image. Structure thickness will, however, still be calculated indirectly assuming a specific structure type.

The purpose of this paper is to present a new method for

Correspondence to: Tor Hildebrand. Email: hildebrand@biomed.ee.ethz.ch

the direct estimation of structure thickness without a model-assumption. This is especially important for the analysis of objects with an *a priori* unknown or varying structure type. A recent example illustrating the need for a model-independent thickness estimator is the study of changes in the structure of trabecular bone undergoing remodelling (Kinney *et al.*, 1995). The authors found that it was pointless to compare an indirectly derived mean trabecular thickness of the initial measurements with that of the subsequent measurements because bone remodelling changed the type of the structure too radically, from a plate-like to a rod-like structure.

The method described in this work estimates a volume-based local thickness by fitting maximal spheres to every point in the structure. From these local thicknesses a volume-weighted mean thickness and the thickness distribution are calculated. A similar method for 2-D sections was developed for the calculation of the mean trabecular plate thickness (Garrahan *et al.*, 1987). With this method, local apparent widths are calculated by fitting circles to the sectioned structure. The mean plate thickness is then calculated indirectly from the apparent width using stereological considerations.

The thickness definition presented differs from the conventional surface-based ones, in which a local thickness is defined for every point on the surface as the orthogonal distance to the opposite surface. The reason for introducing a volume-based local thickness is that a surface-based definition tends to overestimate thickness when arbitrary and nonideal structures are being analysed. An analogous situation has arisen in the quantification of anisotropy; Odgaard *et al.* (1990) found that a volume-based estimator of anisotropy corresponds better with perceived orientation than does a surface-based one.

First the thickness definition used is explained, and the general theory for the calculation of the mean value and distribution is given, followed by practical modifications for the discrete implementation (Section 2). In Section 3 the new method is applied to trabecular bone which was measured with a 3-D micro-CT system.

2. Definitions and methods

2.1. Local and mean thickness

From a general thickness definition we expect that primitive geometrical objects like plates, cylinders or balls are adequately described, i.e. for a plate with thickness d, a cylinder and a ball with diameter d, the thickness according to the definition should be d. For an arbitrary structure the thickness should correspond well with the intuitive conception of thickness as the dimension through an object, as opposed to length or width. Another requirement is a well-defined weighting of the mean value, allowing

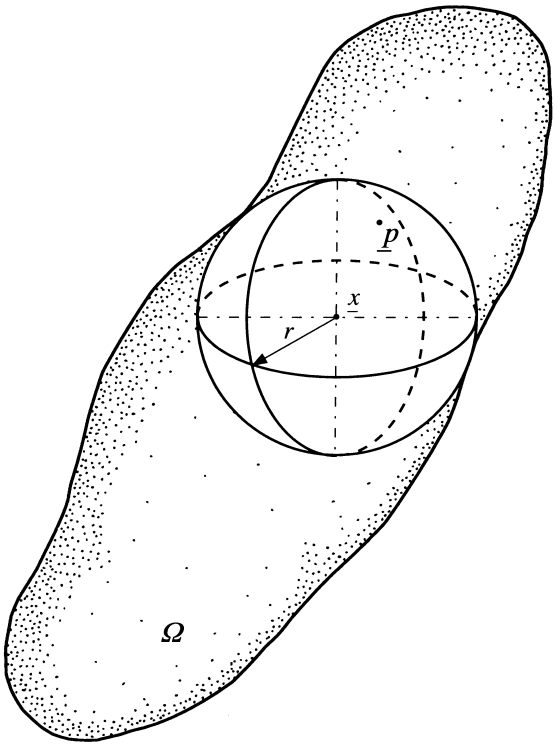

Fig. 1. Local thickness $\tau(\underline{p})$ of a structure Ω determined by fitting maximal spheres to the structure.

unique mean values for objects with varying structure thickness or objects with a compound structure type. To achieve this we propose a new definition of local structure thickness. Let $\Omega \subset \mathbf{R}^3$ be the set of all points of the spatial structure under study and $\underline{p} \in \Omega$ an arbitrary point in this structure. As the local thickness $\tau(\underline{p})$ we define the diameter of the largest sphere which contains the point $(\underline{p})$ and which is completely inside the structure (Fig. 1):

$$\tau(\underline{p}) = 2 \cdot \max(\{r | \underline{p} \in \mathrm{sph}(\underline{x}, r) \subseteq \Omega, \underline{x} \in \Omega\}) \qquad (1)$$

where $\mathrm{sph}(\underline{x},r)$ is the set of points inside a sphere with centre $\underline{x}$ and radius r. In the case of an ideal cylinder with infinite length, for example, all points in the structure will have the same local thickness value corresponding to the diameter of the cylinder.

Since the local thickness is defined for all points of the 3-D structure we will refer to it here as a volume-based local thickness.

As the mean thickness of the structure we define the arithmetic mean value of the local thicknesses taken over all points in the structure:

$$\bar{\tau} = \frac{1}{\mathrm{Vol}(\Omega)} \iiint_{\Omega} \tau(\underline{x}) \mathrm{d}^3\underline{x}, \quad \mathrm{Vol}(\Omega) = \iiint_{\Omega} \mathrm{d}^3\underline{x}. \qquad (2)$$

The maximal local thickness is equivalent to the diameter of

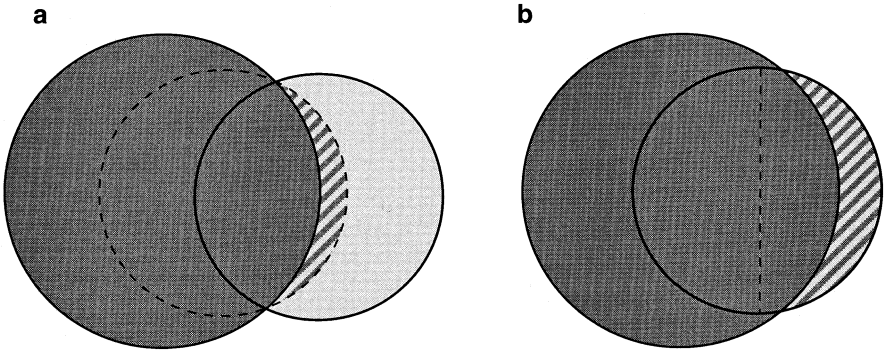

Fig. 2. Local thicknesses of two intersecting balls of different diameter $d_1 < d_2$. (a) The concatenated object has a local thickness equal to d_2 in the region corresponding to the larger ball (dark shaded) in all stages of intersection, whereas the remaining region of the smaller ball has a local thickness continuously changing from d_2 to d_1 in a transition zone (dashed) and constant local thickness d_1 in the right most part. (b) If the intersection goes beyond the meridian (perpendicular to the drawing) of the smaller ball, the transition zone will completely fill out the protruding region in the smaller ball.

the largest sphere that completely fits inside the structure

$$\tau_{\max} = \max(\{\tau(\underline{p}) | \underline{p} \in \Omega\}). \qquad (3)$$

The proposed thickness definition for a structure can also be applied to the structure background or the nonstructure parts of the region examined. The thickness of the background can be interpreted as the width of cavities in the structure or as the distance between structures. It can thus be used to estimate parameters like the mean diameter of channels going through a structure or the mean diameter of spherical voids in a structure. Another possible usage is the assessment of plate or membrane separation.

2.2. Thickness distribution

The mean thickness calculation in (2) corresponds to a *volume-weighted* thickness distribution. Let the point X be a random variable with realizations in Ω, uniformly distributed and $T = \tau(X)$ the local thickness at this point. Then the derived random variable T has the following probability distribution function:

$$F(\tau) = \frac{\mathrm{Vol}(\Omega_\tau)}{\mathrm{Vol}(\Omega)}, \quad \Omega_\tau = \{\underline{x} \in \Omega | \tau(\underline{x}) \leq \tau\}. \qquad (4)$$

The mean thickness in (2) can also be calculated indirectly from the distribution (4), giving the same value. Using the thickness distribution, higher moments of T can be calculated. The kth central moment of T may be written as

$$\Psi_k = \mathbf{E}[(T - \bar{\tau})^k] = \int_0^{\tau_{\max}} (\tau - \bar{\tau})^k \mathrm{d}F(\tau). \qquad (5)$$

Of special interest is the thickness variation, which can be quantified by the standard deviation calculated as the square root of the second central moment ($\sqrt{(\Psi_2)}$). Skewness and kurtosis of the distribution are further measures that can be derived from higher moments (3rd and 4th). The central moment values can be used for a better separation or classification of different structure types when no significant differences can be found in the mean values.

2.3. Interpretation and discussion

It is evident that the proposed mean thickness definition gives the desired values for the above-mentioned standard geometrical objects (plate, cylinder, ball). To understand the character of the mean value in a more general case, the interpretation and the validity of the mean thickness of some simplified nonideal objects are discussed.

An important property of a thickness estimator is its behaviour when objects of different sizes intersect. This can be examined by considering two balls of different diameters $d_1 < d_2$ (Fig. 2a). The local thickness of the joint structure is equal to d_2 in the region of the larger ball. In the remaining region corresponding to the protruding part of the smaller ball, the local thickness continuously changes from d_1 to d_2 in a *transition zone*. The transition zone completely fills out the protruding part of the smaller ball if less than half of its surface is visible (Fig. 2b). The interpretation of the mean thickness of joint structures is somewhat more complicated: if a large ball is hit by several smaller balls (Fig. 3b) then the mean thickness of the joint structure can be smaller than the diameter of the large ball. This may contradict the intuitive expectation. For an interpretation of this case, the situation before intersection is considered (Fig. 3a): the weighted mean thickness of the unconnected structure is smaller than that of the intersected structure. The more the small balls intersect with the larger one, the closer the mean value will come to its diameter (Fig. 3c). Hence, the definition sees the small balls as thinner parts of the compound structure and weights their local thicknesses according to their volume fraction. If, however, the smaller balls form an additional connected layer to the larger ball, the mean thickness can indeed be larger than d_2 (Fig. 3d).

The behaviour of the mean thickness in the previous

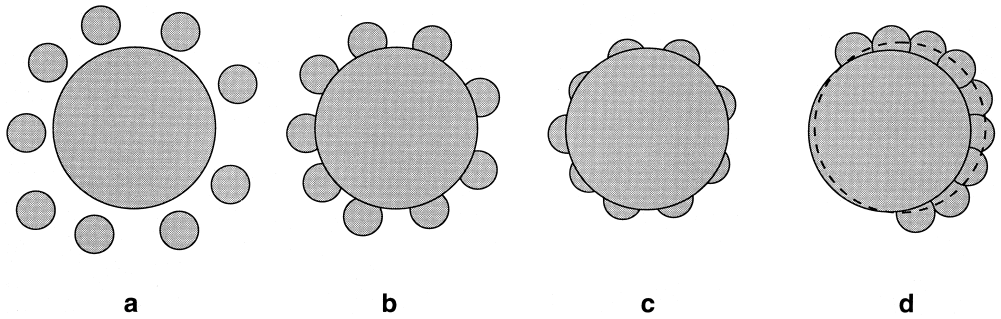

Fig. 3. (a) The mean thickness of a structure consisting of one large ball and several smaller ones is the volume-weighted mean of the diameters. (b) If the small balls intersect with the larger one, the mean thickness for the compound structure increases owing to the reduced volume weight of the small balls. (c) The more the small balls intersect with the large one, the more the mean thickness approaches the diameter of the large ball. (d) The mean thickness exceeds the diameter of the large ball only if the intersecting small balls form an additional connected layer. The dashed line indicates the new maximal sphere which fits the structure in such a situation.

example can be a problem if structures with rough surfaces are examined. In such cases, the attempt to measure small features at the surface will lead to an undesirable underestimation of the mean thickness. In many situations, however, there is *a priori* knowledge regarding the biological range of the examined structure's dimensions and it is possible to define a minimal structure thickness $T_{\min}$ which is yet larger than the extent of the surface roughness. A corrected mean thickness can then be calculated using the probability distribution function (4):

$$\bar{\tau} = \frac{1}{1 - F(T_{\min})} \int_{T_{\min}}^{\tau_{\max}} \tau \, \mathrm{d}F(\tau). \qquad (6)$$

It is worth noting that the part of the structure taken into consideration in (6) composes the smoothed structure actually being described by the corrected mean value. An equivalent technique (Stenberg, 1980) was in fact used to smooth 3-D surfaces defined by 2-D grey-value images by fitting spheres with a fixed diameter (equivalent to $T_{\min}$) to the corresponding structure of the surface.

In the practical use of morphometric methods edge effects are to be considered. Edge effects arise at the boundaries of regions being analysed, where the structure is cut. This leads to a distorted, finite structure with 'unnatural' sharp edges, which will bias the morphometric parameters derived from the structure. For example, a finite cylinder will, according to the thickness definition, be treated as a cylinder with rounded edges and with additional caps at each end, containing the sharp edges (Fig. 4). In all points of the rounded cylinder the local thickness is equal to the diameter of the cylinder. In the caps the local thickness will gradually decrease to zero at the corners of the sharp edges. As a consequence, the mean thickness is slightly smaller than the diameter of the cylinder. This effect can only partly be rectified with the corrected mean value in (6) by disregarding the unlikely small local thicknesses close to the edges. A more reliable correction of edge effects can be achieved by reducing the region of interest in (2) and (4) subsequent to the local thickness determination by moving all boundaries inwards by a distance equal to a predefined maximal possible thickness $T_{\max}$ of the structure being analysed. The boundary-influenced local thicknesses will not therefore be considered in the calculation of the mean value and the distribution. Again, *a priori* knowledge is required to define a tissue-dependent constant. In contrast to a minimal thickness, a reasonable value for $T_{\max}$ can be selected quite easily, by deriving the parameter $\tau_{\max}$ from a representative set of structure samples. This technique is similar to the one used by the estimation of numerical density (Gundersen, 1977), in which 'unbiased test frames' are used to suppress edge effects.

The proposed definition of the local thickness differs from the one used for plates or barriers, in which the local thickness is defined for all points on the structure surface as the shortest distance to the opposite surface (Cruz-Orive, 1979; Weibel, 1980). For objects with a joint surface

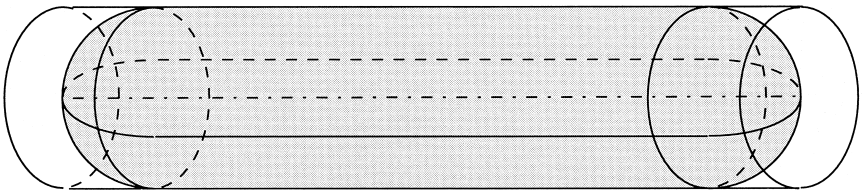

Fig. 4. Mean thickness of a finite cylinder: if the edges are perfectly rounded (shaded) the mean thickness is equal to the diameter of the cylinder. An abruptly cut cylinder will be treated as a cylinder with rounded edges and with an additional cap containing the 'thinner' sharp edge. As a consequence the mean thickness would be smaller than the diameter of the cylinder.

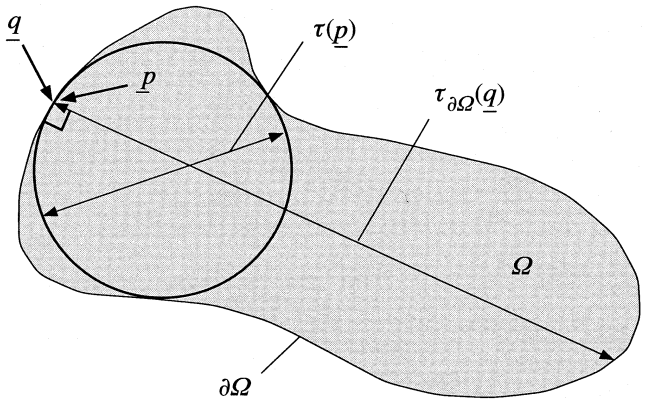

Fig. 5. Difference between the proposed volume-based and a surface-based local thickness. Let $\partial\Omega \subset \mathbf{R}^3$ be the set of all points on the surface of the structure and $\underline{q} \in \partial\Omega$ an arbitrary point on the surface. The surfaced-based local thickness $\tau_{\partial\Omega}(\underline{q})$ is the orthogonal distance to the opposite surface. The volume-based local thickness at this point but just inside the structure ($\underline{p} \in \Omega$) is shown with its appertaining sphere. (A 2-D section of the structure is shown for clarity.)

(cylinders or spheres) the orthogonal distance from the surface to the opposite surface is used because there is no clearly defined shortest distance. For some ideal geometrical structures (the three previously mentioned primitive geometrical objects included) the surface-based thickness is equal to the proposed volume-based thickness. For an arbitrary structure, however, the orthogonal distance from a point on the surface need not necessarily correspond with the intuitive thickness associated with the point. The example in Fig. 5 shows the difference between the new volume-based thickness definition and the surface-based definition in such a situation. By the calculation of membrane thickness using orthogonal intercepts (Jensen *et al.*, 1979) the local thickness for a point of the surface is defined as the minimal orthogonal distance from the opposite surface back to the point. Here the opposite surface (secondary surface) is assumed disjoint from the surface of the point (primary surface). The object in Fig. 5 is thus not considered as a valid structure by this definition.

The volume-weighted mean thickness implies a mean value calculated with less weight given to thinner parts of a structure. This seems reasonable because the thinner parts describe a smaller portion of the region examined. In special cases, however, a different weighting of the mean value is preferable. A surface-based local thickness implies a surface-weighted mean thickness. This will give barriers of different width and with equal surface area the same influence on the mean thickness, since the surface area is independent of the barrier thickness. When barriers are evaluated with respect to passive transport through the structure material, a harmonic mean thickness is used as a parameter to quantify the permeability of the structure (Weibel, 1980). The harmonic mean thickness is defined as the reciprocal mean of the surfaced-based local thicknesses. To calculate surface-weighted and harmonic mean thickness with the proposed method, it would be possible to extend the volume-based local thickness definition to be valid also on the surface of the structure. To do this a smooth surface must be guaranteed owing to the surface roughness dependency of the local thickness discussed above. Such restrictions are also required in the prevalent surface-based methods: in Cruz-Orive (1979) a sheet structure is considered as the portion of space comprised between two smooth, quasiparallel faces. In Jensen *et al.* (1979) a membrane model with uniformly curved surfaces was assumed. A more general smoothness assumption is used by Sandau (1993), in which the thickness of 'flat bodies' is estimated from measurements on vertical sections. Flat bodies were mathematically described by a stationary weighted surface process in which a joint distribution of spatial direction and thickness exist.

2.4. Discrete implementation

The thickness definition described assumes a continuously represented structure. Since this is not achievable with a conventional 3-D measuring system, it is important to be able to use the method on discretized images. Typically, a segmented image is described by binary cubic voxels indicating structure or background. The voxel volume is thus used as a geometrical approximation of the true 3-D structure. It must therefore be ensured that the resolution of the measuring system is sufficient for the structure being examined. The sharp edges of the cubic voxels give the structure a rough surface which implies the use of Eq. (6) for the calculation of mean thickness. A minimal value for the constant $T_{\min}$ should thereby be larger than the dimension of a voxel.

For the practical implementation the compact formulation of the local thickness in (1) may be subdivided into more manageable expressions. This can be achieved by expressing (1) in terms of the structure *distance map* (see Danielsson, 1980; Serra, 1988). The distance map (D_{map}) is calculated by the distance transformation, assigning to every point in the structure the Euclidean distance from that point to the nearest background point; this is equivalent to the radius of the largest sphere centred at the point and still completely inside the structure. The distance transformation is defined as

$$D_{\text{map}}(\underline{q}) = \max(\{r > 0 | \text{sph}(\underline{q}, r) \subseteq \Omega\}), \quad \underline{q} \in \Omega. \qquad (7)$$

The local thickness can now be rewritten using the distance map

$$\tau(\underline{p}) = 2 \cdot \max_{\underline{q} \in X(\underline{p})} (D_{\text{map}}(\underline{q})) \qquad (8)$$

where the set $X(\underline{p})$ represents the centre points of all spheres with a radius equal to their corresponding distance value

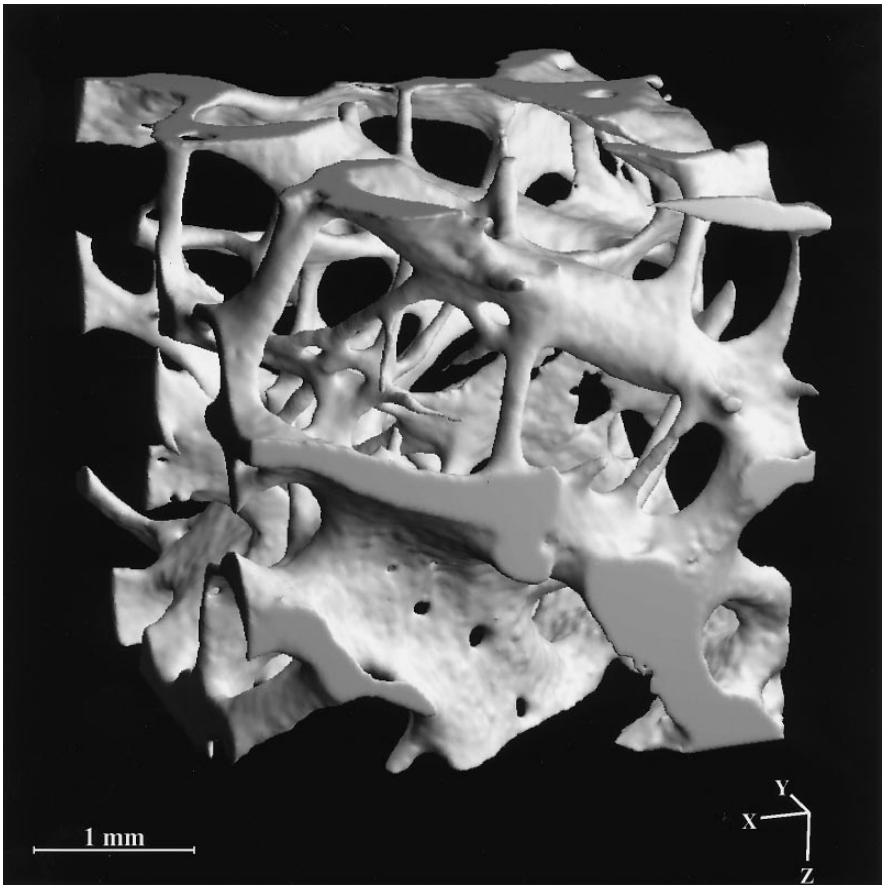

Fig. 6. Trabecular bone structure from the human iliac crest. The VOI represents a region of $4 \times 4 \times 4$ mm^3 ($286 \times 286 \times 286$ voxels) from an 8-mm cylindrical core. The estimated mean thickness of the structure is 0·20 mm with a standard deviation of 0·11 mm.

and including the point $\underline{p}$:

$$X(\underline{p}) = \{\underline{x} \in \Omega | \underline{p} \in \mathrm{sph}(\underline{x}, D_{\mathrm{map}}(\underline{x}))\}. \quad (9)$$

The calculation of the local thickness is thereby split into two steps. The first step is the calculation of the distance map, which can be carried out efficiently on discrete data because the fitting of spheres in (7) in one point is independent of the neighbour points and therefore suitable for parallel processing. With a 3-D extension of iterative methods for 2-D data (Yamada, 1984), the distance transformation can also be calculated in an acceptable time on sequential computers (Borgefors, 1984; Saito & Toriwaki, 1994).

The implementation of the second step would lead to massive computational overhead if carried out directly according to (8) owing to the sphere inclusion tests in (9). By defining the distance ridge as the set of the centre points of all nonredundant spheres,

$$\Omega_R = \{\underline{p} \in \Omega | \mathrm{sph}(\underline{p}, D_{\mathrm{map}}(\underline{p})) \not\subseteq \mathrm{sph}(\underline{x}, D_{\mathrm{map}}(\underline{x})), \underline{p} \neq \underline{x}, \underline{x} \in \Omega\} \quad (10)$$

it is only necessary to check for the corresponding spheres in these points by redefining the set (9) used in (8) by

$$\tilde{X}(\underline{p}) = \{\underline{x} \in \Omega_R | \underline{p} \in \mathrm{sph}(\underline{x}, D_{\mathrm{map}}(\underline{x}))\}. \quad (11)$$

The necessary additional calculation of the distance ridge can therefore be done efficiently on discrete data by making the inclusion test in (10) locally for the neighbour voxels only. Such a technique does not necessarily exclude all redundant points, but the preservation of the nonredundant points is always ensured. The distance ridge corresponds to the medial axis of a structure (see Goldak *et al.*, 1991), but it does not represent a topological skeleton when derived from a voxel image. This is, however, insignificant for the method described here because the distance ridge is not used for connectivity measures.

The accuracy of the method when applied to discrete data depends on the resolution of the image acquisition system used. The local thickness will have a stochastic error corresponding to the dimension of one voxel. In the case of poor image quality, possible noise structures will influence the local thickness determination and will lead to an underestimation of the actual thickness. This problem can be treated in the same way as the effect of rough surfaces (see Section 2.3).

3. An example of application: trabecular bone measured with microcomputed tomography

3.1. Trabecular bone structure

Trabecular bone is an example of a structure with varying architecture. The actual structure depends on the type of

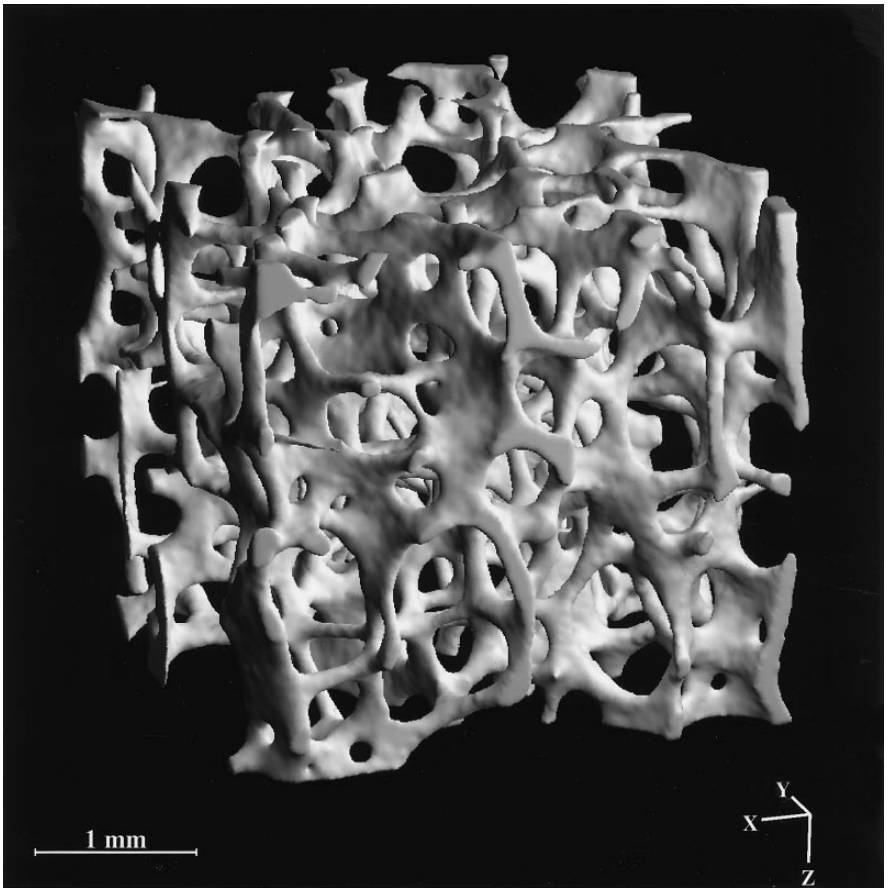

Fig. 7. Trabecular bone structure from the second lumbar vertebra of the human spine. The estimated mean thickness of the structure is 0·11 mm with a standard deviation of 0·03 mm.

bone examined, the location of the sample in the bone and also on age, sex and diseases of the donor. This makes it unsuitable to use methods which assume a fixed structure model to derive morphometrical parameters, when samples with an *a priori* unknown architecture are examined.

3.2. The μCT measuring system

We used a newly developed high-resolution microcomputed tomograph (μCT) to measure bone biopsies nondestructively (Rüegsegger *et al.*, 1996). The system is based on a compact fan-beam-type CT scanner that can work in spiral scanning or multislice mode. An X-ray tube with a microfocus is used as a source, a CCD-array as a detector. Typically, bone biopsies with a diameter of 8 mm and a length of up to 36 mm are measured. Spatial resolution is 28 μm and the voxel size is $14 \times 14 \times 14$ μm^3. The 3-D grey-level image thus measured can be segmented and displayed with 3-D image processing techniques (Müller *et al.*, 1994).

3.3. Evaluation of structure thickness

Two fresh human bone biopsies from the iliac crest and the lumbar spine were measured with the above-described μCT system. From each measurement a cubic volume of interest (VOI) was selected and processed, resulting in a 3-D binary image with 286^3 voxels, corresponding to physical dimensions of 4 mm $\times$ 4 mm $\times$ 4 mm. In both bone samples the structure volume fraction is about 12%.

Three-dimensional visualizations of the two measured samples are shown in Fig. 6 and Fig. 7. The thickness distributions of the structures were calculated using algorithms described in Section 2.4. The total processing time for the analysis of one sample on a DEC 3000 M500 AXP was less than 15 min. The processing modules, including procedures for segmentation and analysis, are built into a software package called IPL (Image Processing Language) which allows full automatic processing without any operator interaction. The resulting thickness distributions of the two samples are shown in Fig. 8 (the probability density function is used for clarity).

The derived thickness distributions correspond well with the structure characteristics observed in the 3-D visualizations: in the case of the iliac crest sample (Fig. 6) a large variation of structure thickness can be seen; thick plates with a maximal thickness of 0·6 mm are interconnected by thin rods with a diameter of about 0·1 mm. The appertaining distribution is wide with a mean value of 0·20 mm and a standard deviation of 0·11 mm. In the lumbar spine sample (Fig. 7) a homogenous structure with

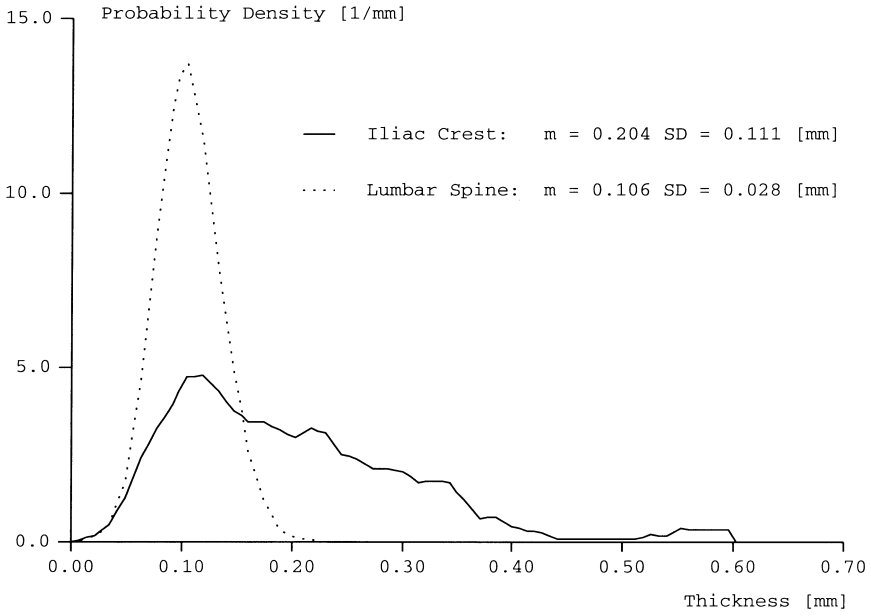

Fig. 8. Thickness distributions of trabecular bone structures from the iliac crest and the lumbar spine derived from the volume-based local thickness.

plates and rods with almost constant thicknesses can be observed. The distribution in this case is a narrow peak with a mean value of 0·11 mm and a standard deviation of 0·03 mm.

4. Conclusions

The new method for a direct thickness determination of 3-D structures is founded on a volume-based local thickness definition. We define local thickness at a given point in the structure as the diameter of the largest sphere which includes the point and which can be fitted completely inside the structure.

Since the method is not model based, assumptions on the structural type are no longer necessary. Thus it is possible to assess a mean thickness of any structure and even to quantify thickness changes in structures undergoing architectural remodelling.

An important feature of the method described is the assessment of the thickness distribution. The thickness variability can be quantified using values derived from moments of the distribution, standard deviation and skewness.

Our method requires true 3-D images. In situations in which a 3-D measurement is too time- or resource-consuming for the routine application and in which an unknown but relatively constant structure type can be expected, it should be possible to apply the method described to a small subset of the population examined to calibrate parameters derived with stereological methods from less cumbersome lower-dimensional measurements.

The directly assessed thickness distribution in combination with other 3-D morphometric techniques like volume and surface determination (Guilak, 1994), assessment of anisotropy (e.g. Harrigan & Mann, 1984) and calculation of connectivity (Odgaard & Gundersen, 1993), enables a detailed and versatile quantification of 3-D structures. This information can be used for a better prediction of the quality and functionality of 3-D structures.

Acknowledgment

This work was supported in part by grant 31-29971.90 from the Swiss National Science Foundation.

References

Borgefors, G. (1984) Distance transformation in arbitrary dimensions. *Comp. Vision, Graphics, Image Process.* **27,** 321–345.

Cruz-Orive, L.M. (1979) Estimation of sheet thickness distribution from linear and plane sections. *Biomed. J.* **21,** 717–730.

Cruz-Orive, L.M. & Weibel, E.R. (1990) Recent stereological methods for cell biology: a brief survey. *Am. J. Physiol.* **258,** L148–L156.

Danielsson, P.E. (1980) Euclidean distance mapping. *Comp. Graphics Image Process.* **14,** 227–248.

Feldkamp, L.A., Goldstein, S.A., Parfitt, A.M., Jesion, G. & Kleerekoper, M. (1989) The direct examination of three-dimensional bone architecture *in vitro* by computed tomography. *J. Bone Min. Res.* **4,** 3–11.

Garrahan, N.J., Mellish, R.W.E., Vedi, S. & Compston, J.E. (1987) Measurement of mean trabecular plate thickness by a new computerized method. *Bone,* **8,** 227–230.

Goldak, J.A., Xinhua, Y., Knight, A. & Lingxian, D. (1991) Constructing discrete medial axis of 3-d objects. *Int. J. Comput. Geom. Appl.* **1,** 327–339.

Guilak, F. (1994) Volume and surface area of viable chondrocytes *in situ* using geometric modeling of serial confocal sections. *J. Microsc.* **173,** 245–256.

Gundersen, H.J.G. (1977) Notes on the estimation of the numerical density of arbitrary profiles: the edge effect. *J. Microsc.* **111,** 219–223.

Gundersen, H.J.G., Bagger, P., Bendtsen, T.F., Evans, S.M., Korbo, L., Marcussen, N., Møller, A., Nielsen, K., Nyengaard, J.R., Pakkenberg, B., Sørensen, F.B., Vestersby, A. & West, M.J. (1988a) The new stereological tools: disector, fractinator, nucleator and point sampled intercepts and their use in pathological research and diagnosis. *APMIS*, **96,** 857–881.

Gundersen, H.J.G., Bendtsen, T.F., Korbo, L., Marcussen, N., Møller, A., Nielsen, K., Nyengaard, J.R., Pakkenberg, B., Sørensen, F.B., Vestersby, A. & West, M.J. (1988b) Some new, simple and efficient stereological methods and their use in pathological research and diagnosis. *APMIS*, **96,** 379–394.

Gundersen, H.J.G., Jensen, T.B. & Østerby, R. (1978) Distribution of membrane thickness determined by lineal analysis. *J. Microsc.* **113,** 27–43.

Harrigan, T.P. & Mann, R.W. (1984) Characterization of microstructural anisotropy in orthotropic materials using a second rank tensor. *J. Mater. Sci.* **19,** 761–767.

Jara, H., Wehrli, F.W., Chung, H. & Ford, J.C. (1993) High-resolution variable flip angle 3D, MR imaging of trabecular microstructure *in vivo*. *Magn. Reson. Med.* **29,** 528–539.

Jensen, E.B., Gundersen, H.J.G. & Østerby, R. (1979) Determination of membrane thickness distribution from orthogonal intercepts. *J. Microsc.* **115,** 19–33.

Kinney, J.H., Lane, N.E. & Haupt, D.L. (1995) In vivo, three-dimensional microscopy of trabecular bone. *J. Bone Miner. Res.* **10,** 264–270.

Müller, R., Hildebrand, T. & Rüegsegger, P. (1994) Non-invasive bone biopsy: a new method to analyse and display the three-dimensional structure of trabecular bone. *Phys. Med. Biol.* **39,** 145–64.

Odgaard, A. & Gundersen, H.J.G. (1993) Quantification of connectivity in cancellous bone, with special emphasis on 3-D reconstructions. *Bone*, **14,** 173–182.

Odgaard, A., Jensen, E.B. & Gundersen, H.J.G. (1990) Estimation of structural anisotropy based on volume orientation. A new concept. *J. Microsc.* **157,** 149–162.

Rüegsegger, P., Koller, B. & Müller, R. (1996) A microtomographic system for the non-destructive evaluation of bone architecture. *Calcif. Tiss. Int.* **58,** 24–29.

Saito, T. & Toriwaki, J.I. (1994) New algorithms for euclidean distance transformation of an *n*-dimensional digitized picture with applications. *Pattern Recognition*, **27,** 1551–1565.

Sandau, K. (1993) An estimation procedure for the joint distribution of spatial direction and thickness of flat bodies using vertical sections, Part I: theoretical considderations. *Biomed. J.* **35,** 649–660.

Serra, J. (1988) *Image Analysis and Mathematical Morphology*, Vol. 2. Academic Press, London.

Stenberg, S.R. (1980) Language and architecture for parallel image processing. *Pattern Recognition in Practice* (ed. by E. S. Gelsema and L. N. Kanal), pp. 35–44. North-Holland, Amsterdam.

Weibel, E.R. (1963) Principles and methods for the morphometric study of the lung and other organs. *Lab. Invest.* **12,** 131–155.

Weibel, E.R. (1980) *Stereological Methods, Vol. 2: Theoretical Foundations*. Academic Press, London.

Weibel, E.R. & Knight, B.W. (1964) A morphometric study on the thickness of pulmonary air–blood barrier. *J. Cell Biol.* **21,** 367–384

Whitehouse, W.J. (1974) The quantitative morphology of anisotropic trabecular bone. *J. Microsc.* **101,** 153–168.

Wijnaends van Resandt, R.W., Marsman, H.J.B., Kaplan, R., Davoust, J., Stelzer, E.K.H. & Stricker, R. (1985) Optical fluorescence microscopy in three dimensions: microtomoscopy. *J. Microsc.* **138,** 29–34.

Wilson, T. (ed.) (1990) *Confocal Microscopy*, pp. 1–60. Academic Press, London.

Yamada, H. (1984) Complete euclidean distance transformation by parallel operation. *Proc. 7th Int. Conf. on Pattern Recognition, Canada*, pp. 69–71. IEEE Computer Society Press, Silver Spring, MD, U.S.A.